

Step structure and ordering in Zn-doped GaInP

S. H. Lee, C. M. Fetzer, and G. B. Stringfellow^{a)}

Department of Materials Science and Engineering, University of Utah, Salt Lake City, Utah 84112

C.-J. Choi and T. Y. Seong

Department of Materials Science and Engineering, Kwangju Institute of Science and Technology, Kwangju 506-712, Korea

(Received 4 December 1998; accepted for publication 5 May 1999)

GaInP grown on (001) substrates by organometallic vapor phase epitaxy is typically highly ordered. The driving force is due to the $[\bar{1}10]$ oriented P dimers on the surface. There are apparently additional kinetic factors related to surface steps that also play a key role in the ordering mechanism. However, the mechanism remains undetermined. This work presents the effects of Zn on the step structure and ordering during epitaxial growth. The degree of order is estimated from the low temperature photoluminescence peak energy to be approximately 0.5 for undoped epitaxial layers and the layers are completely disordered at Zn doping concentrations [from dimethylzinc (DMZn) addition to the system] of $> 1.7 \times 10^{18} \text{ cm}^{-3}$. This is verified by transmission electron diffraction results. As a consequence, the band gap energy increases by 110 meV as the Zn doping level is increased from 3×10^{17} to $1.7 \times 10^{18} \text{ cm}^{-3}$. The $[\bar{1}10]$ and $[110]$ -step spacing as well as the root-mean-square roughness are found to be unchanged over the range of doping that produces disordering for both singular (001) and vicinal substrates. This indicates the disordering mechanism induced by Zn does not involve the step edge adatom attachment kinetics as previously reported for Te. The disordering is believed to be caused by the intermixing of Ga and In due to the increase in diffusion coefficient caused by the introduction of Zn. Modulation of the DMZn flow rate during growth has been used to grow heterostructures and quantum wells. No well boundaries were observed by transmission electron microscopy for thin wells, although both ordered and disordered regions are observed in 50 nm "wells." This is believed to result from Zn diffusion between the layers during growth. © 1999 American Institute of Physics. [S0021-8979(99)02116-7]

INTRODUCTION

Atomic-scale ordering to produce the CuPt structure frequently occurs in $\text{Ga}_{0.52}\text{In}_{0.48}\text{P}$ layers grown by organometallic vapor phase epitaxy (OMVPE) on (001)-oriented GaAs substrates.¹ The Ga and In atoms are spontaneously segregated into alternating $\{111\}$ monolayers. Theoretically, for vapor phase epitaxy on (001)-oriented substrates, the alternating surface stresses resulting from the formation of rows of $[\bar{1}10]$ -oriented phosphorous dimers on the $(2 \times n)$ reconstructed (001) surface thermodynamically stabilize the variants of the CuPt structure with ordering on the $(\bar{1}11)$ and $(1\bar{1}1)$ planes.^{1,2}

This phenomenon is of considerable practical interest since ordering has a large effect on the materials properties, e.g., the band gap energy is found to be 160 meV lower in partially ordered $\text{Ga}_{0.52}\text{In}_{0.48}\text{P}$ than in disordered material of the same composition.³ This is very important for visible light emitting diodes and injection laser diodes. Ordering must be avoided in order to produce the shortest wavelength devices. On the other hand, ordering offers the possibility of producing heterostructures by changing the band gap energy without altering the solid composition.³

The driving force for ordering is understood, but the mechanism remains unknown even though several speculative models have been proposed.⁴ Surface steps appear to

play a key role in the ordering process. For example, as the growth temperature is increased from 520 to 670 °C,^{5,6} the average step height (bilayer versus monolayer) and the degree of order change simultaneously. In addition, $[\bar{1}10]$ steps are observed to assist the ordering process but $[\bar{1}10]$ steps retard ordering.⁷ These results indicate that kinetic effects at step edges affect the ordering process under certain growth conditions. Earlier work has probed the ordering mechanism using observations of changes in growth parameters known to affect the degree of order on the step structure.^{5,6}

One of the factors having a strong effect on ordering is doping. Several studies in GaInP have demonstrated a connection between ordering and n -type⁸⁻¹² or p -type¹³⁻¹⁹ dopant concentration. The results show that a drastic decrease in ordering (or increase in band gap energy) is caused by introducing a high concentration of dopants during OMVPE growth. Recently, it was found that with increasing Te concentration at levels of $> 3 \times 10^{17} \text{ cm}^{-3}$, during OMVPE growth of GaInP on nominally (001) oriented substrates, the $[\bar{1}10]$ step velocity increased dramatically. The change in step structure was found to coincide with the reduction in the degree of CuPt order.¹⁰⁻¹² This was attributed to the surfactant effects of Te.

For Zn-doped GaInP, highly-doped layers grown by OMVPE were also demonstrated to be disordered by using transmission electron diffraction (TED) or/and photolumi-

^{a)}Electronic mail: stringfellow@coe.utah.edu

nescence (PL) measurements.^{13–16} However, the mechanism for this effect is not understood.

The purpose of this article is to present the results of a study of Zn dopant effects on both step structure and ordering in GaInP in an effort to further clarify the disordering mechanism, in particular to compare the results obtained for Zn with those reported earlier for Te. Above a Zn concentration of 10^{18} cm^{-3} , a sharp drop in the degree of order is observed. This doping level is considerably higher than the value observed to cause disordering using Te. By using atomic force microscopy (AFM), the surface morphology and step structure were observed to be nearly unchanged over the range of doping that produces disordering, in sharp contrast to the results for Te doping. This suggests that the disordering mechanism is entirely different.

EXPERIMENT

Zn-doped GaInP layers were grown by OMVPE in a horizontal, infrared-heated, atmospheric-pressure reactor using trimethylindium, trimethylgallium, and tertiarybutylphosphine, with dimethylzinc (DMZn) as the dopant precursor on semi-insulating GaAs substrates having both singular (001) and vicinal (3° toward (111)B direction or 3°_B) orientations. The DMZn was diluted to 472 ppm in H_2 . The carrier gas was Pd-diffused hydrogen. The total flow rate was 4360 sccm. Substrates were prepared by degreasing followed by a 1 min etch in a 2:12:1 solution of NH_4OH , H_2O , and H_2O_2 . Before beginning the GaInP growth, a $0.05 \mu\text{m}$ GaAs buffer layer was deposited to improve the quality of the GaInP layer. The GaInP thickness was about $0.3 \mu\text{m}$ for all samples. The growth rate was $0.6 \mu\text{m/h}$ and the growth temperature was 670°C . The TBP partial pressure and V/III ratio were kept constant at 3.0 Torr and 180, respectively. After completing the growth, the group III precursors were removed and the samples were cooled rapidly.

The free electron concentrations and mobilities were determined from room temperature Hall effect measurements using the Van der Pauw geometry. Ohmic contacts were formed using In/Zn dots alloyed for 10 min at 300°C in N_2 . The composition of the GaInP layers was determined using Vegard's law from x-ray diffraction measurements using $\text{Cu } K_\alpha$ radiation. Only results for lattice-matched layers, with values of GaP concentration in the solid of 0.515, are presented here. The 20 K PL was excited with the 488 nm line of an Ar^+ laser. The emission was dispersed using a Spex Model 1870 monochromator and detected using a Hamamatsu R1104 head-on photomultiplier tube. [110] cross-sectional transmission electron microscope (TEM) samples were prepared using standard Ar^+ ion milling at 77°K . The TED patterns were obtained using a JEM 2010 instrument operated at 200 KV. The thicknesses of the thin foils examined by TEM were mostly in the range from 150 to 400 nm.

The surface structure was characterized using a Nanoscope III AFM in the tapping mode. Etched single-crystalline Si tips were used with an end radius of about 5 nm, with a sidewall angle of about 35° . Scan rates of 1 to 2 lines per second were used and data were taken at 512 points/line and

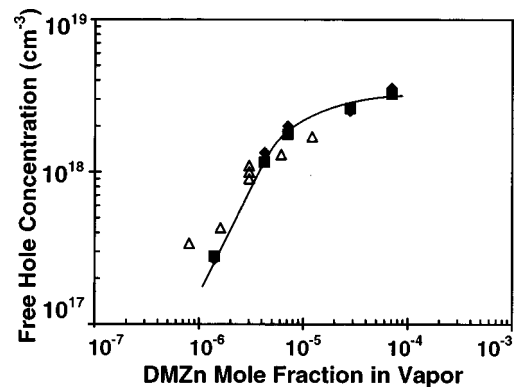


FIG. 1. Hole concentration vs mole fraction of DMZn in the vapor: GaInP (001) singular (\blacklozenge) and vicinal (3° toward (111)B) layers (\blacksquare) were grown at 670°C . Data points (\triangle) for Zn-doped GaInP (001) layers grown at 680°C from Ikeda and Kaneko (see Ref. 21) are shown for comparison. The solid line is a best fit through the data from this work.

512 lines per scan area. The samples were measured in air, so were covered by a thin, conformal oxide layer.

RESULTS

Figure 1 shows that the free hole concentration is proportional to the DMZn flow rate for doping levels $\leq 1.3 \times 10^{18} \text{ cm}^{-3}$, while the hole concentration becomes sublinear for higher doping levels and saturates at a hole concentration of approximately $3 \times 10^{18} \text{ cm}^{-3}$. The doping for vicinal layers is very nearly that for singular (001) layers for the same growth conditions. This is similar to results for Zn-doped and Mg-doped AlGaInP layers in which no significant doping changes were reported for misorientation from (001) by a few degrees toward (111)B.²⁰ Data for Zn doping of (001) GaInP layers from Ikeda and Kaneko²¹ are shown in Fig. 1 for comparison with the present data, although the growth temperature was reported to be 680°C versus 670°C for this work.

In the linear range, the Zn distribution coefficient, k_{Zn} , defined as the ratio of hole concentration to the concentration of group III lattice sites divided by the ratio of the DMZn concentration to the group III concentration in the vapor phase,²² is 3.8×10^{-4} for the singular (001) substrates and 3.3×10^{-4} for 3°_B substrates, at a doping level of 10^{18} cm^{-3} . These values are consistent with the literature values of 1.5×10^{-3} at 640°C ²³ and 2×10^{-4} at 680°C ²¹ for layers grown by OMVPE since Zn doping is known to decrease as the growth temperature is increased.²⁴

Figure 2 shows the PL peak energy versus the Zn doping level for both singular and vicinal substrates. The degree of order, S , was deduced from the 20 K PL peak energy for GaInP layers lattice matched to GaAs using the equation:²⁵

$$S = \{ [2005 - \text{PL peak energy at 20 K (in meV)}] / 471 \}^{1/2}. \quad (1)$$

The value of S is approximately 0.5 for undoped layers ($n \sim 4.8 \times 10^{16} \text{ cm}^{-3}$) and those with low Zn doping levels. The samples become disordered as the Zn concentration exceeds 10^{18} cm^{-3} . The band gap energy changes from 1880 to 1990 meV as the Zn doping level increases from 3×10^{17} to $1.7 \times 10^{18} \text{ cm}^{-3}$.

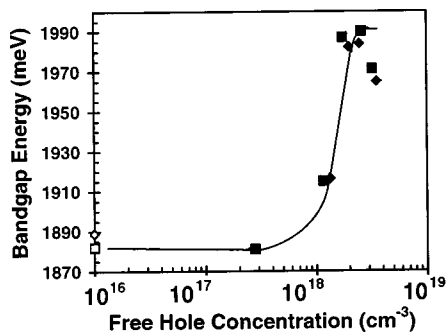


FIG. 2. 20 K PL peak energy vs free hole concentration from Zn doping. GaInP (001) singular (\blacklozenge) and vicinal layers (\blacksquare) were grown at 670 °C. Results for undoped GaInP (001) singular (\diamond) and vicinal layers (\square) are shown for comparison. The undoped GaInP layers have unintentional n -type concentrations of $4.8 \times 10^{16} \text{ cm}^{-3}$ (singular) and $4.2 \times 10^{16} \text{ cm}^{-3}$ (vicinal). The line was simply drawn through the data points.

At doping levels of $\geq 2.6 \times 10^{18} \text{ cm}^{-3}$, which are higher than the doping range that produces disordering, the band gap shrinks due to impurity banding and tailing of states.²⁶ The band gap shrinkage for Zn-doped GaAs with a doping level of $3.3 \times 10^{18} \text{ cm}^{-3}$ at 297 K is approximately 24 meV.²⁷ This can be compared with a band gap shrinkage of ~ 20 meV for Zn-doped GaInP singular and vicinal layers in this work at the same doping level.

It is worthwhile to mention that each PL spectrum consists of two peaks, corresponding to band-to-band and band-to-acceptor transitions, when the hole concentration exceeds $1.3 \times 10^{18} \text{ cm}^{-3}$. Naturally, the highest energy peak was used to determine the band gap energy. The Zn acceptor binding energy in GaInP was measured from the separation of the two peaks to be approximately 30 meV. This can be compared to values of 29,¹⁹ 27,¹⁸ and 24 meV¹⁴ previously reported for Zn-doped GaInP layers.

A more direct, but nonquantitative, measure of the degree of order is provided by TED patterns. Figure 3(a) shows the TED pattern for the Zn-doped GaInP layer with $p = 1.3 \times 10^{18} \text{ cm}^{-3}$ grown on a singular (001) substrate. In addition to the normal zinc-blende lattice spots, extra superspots are observed at the $1/2(\bar{1}11)$ and $1/2(1\bar{1}\bar{1})$ positions, due to the $(\bar{1}11)$ and $(1\bar{1}\bar{1})$ variants of the CuPt structure, typically observed in singular (001) GaInP layers.²⁸ The CuPt superspots have disappeared for a free hole concentration due to Zn doping of $2.0 \times 10^{18} \text{ cm}^{-3}$, as shown in Fig. 3(b). These results are consistent with the quantitative degree of order versus Zn concentration deduced from PL measurements.

Figure 4 shows the surface morphology, measured using the AFM, for several hole concentrations from Zn doping for singular (001) layers. The surface morphology and step structure for low Zn doping layers are very similar to those for undoped layers.²⁹ The step structure is essentially independent of Zn doping level, except at the highest levels of $\geq 2.5 \times 10^{18} \text{ cm}^{-3}$ [e.g., Fig. 4(d)]. The average $[\bar{1}10]$ -step and $[110]$ -step spacings, obtained from a careful counting of the average step spacing along ten $1 \mu\text{m}$ AFM profiles from Fig. 4, are shown in Fig. 5. For $[\bar{1}10]$ steps, the spacing is decreased slightly over the range of doping that produces disordering (i.e., from 3×10^{17} to $1.7 \times 10^{18} \text{ cm}^{-3}$), indicating a slight surfactant effect. For $[110]$ steps, the spacing is

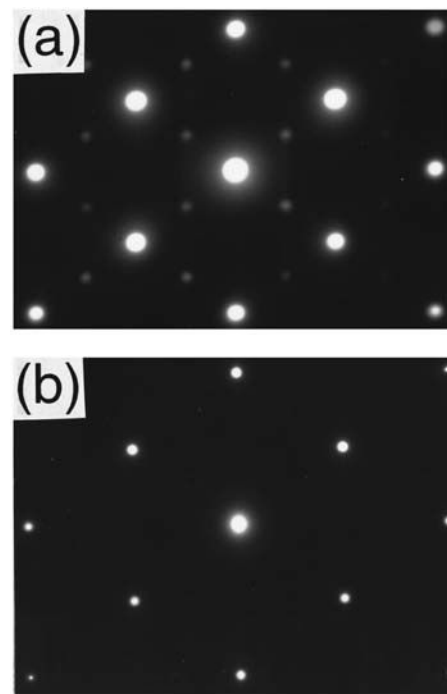


FIG. 3. $[110]$ TED patterns taken from Zn-doped GaInP (001) layers grown at 670 °C: (a) $p = 1.3 \times 10^{18}$ and (b) $p = 2.0 \times 10^{18} \text{ cm}^{-3}$.

found to be unchanged over the entire doping range. In addition, Fig. 6 shows that the root-mean-square (rms) roughness on a $1 \times 1 \mu\text{m}^2$ area is nearly constant for singular (001) and vicinal layers (3°_{B}) except for an increase for the most highly doped singular layer. Indeed, step spacing, step

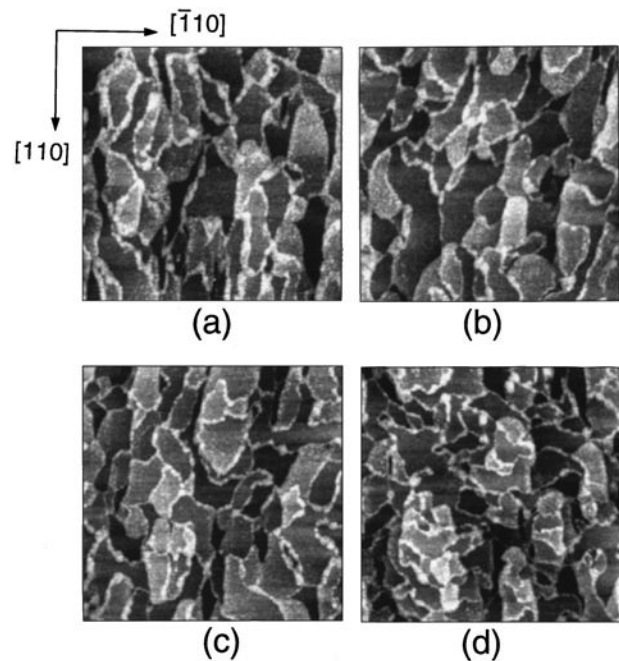


FIG. 4. Surface morphology, measured using the AFM, vs hole concentration from Zn doping for singular (001) layers grown at a temperature of 670 °C. The free hole concentrations are: (a) 2.6×10^{17} (b) 1.3×10^{18} , (c) 2.0×10^{18} , and (d) $2.5 \times 10^{18} \text{ cm}^{-3}$. Note that the surface morphologies and step structures for undoped layers are very similar to those for Zn-doped GaInP layers presented here, except at the highest Zn levels. The scale is $1000 \times 1000 \text{ nm}^2$ for each image.

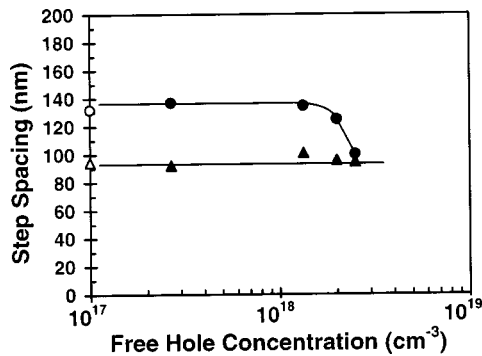


FIG. 5. Step spacing vs free hole concentration for GaInP (001) layers grown at 670 °C with Zn doping (filled symbols) and undoped (open symbols): (●, ○) for [110] steps and (▲, △) for [110] steps. Data for an undoped GaInP layer with an *n*-type concentration of $4.8 \times 10^{16} \text{ cm}^{-3}$ are shown for comparison.

height, and rms roughness are all nearly unchanged over the range of doping that produces disordering. This indicates that, in contrast to the results for Te doping, the disordering mechanism induced by Zn does not involve a change in the adatom sticking coefficients at the step edges.

An attempt was made to produce well structures using a variation of the Zn doping to control the band gap energy. For a single 50 nm “well,” the PL shows strong peaks at 1890 and 1884 meV for singular (001) and vicinal layers, respectively, as shown in Fig. 7. These peaks are believed to originate from the undoped GaInP ordered well layer sandwiched between the GaInP disordered barrier layers with Zn doping levels of $\sim 2 \times 10^{18} \text{ cm}^{-3}$. The amplified spectra at higher photon energies in Fig. 7 show two weak peaks that are nearly the same as the band-to-band and band-to-acceptor peaks obtained from the disordered single layers. Thus, the high energy peaks appear to come from the Zn-doped GaInP barrier layers. This means that the 50 nm wells are not significantly degraded due to Zn diffusion during the growth time. For the 5 nm quantum well (QW), however, the PL energy peak from the thin ordered layer could not be observed. For the 10 nm QW, the PL peak from the ordered layer was barely observed. TEM dark-field images show graded well boundaries for all well structures. These results suggest that the sandwiched ordered layer may become disordered when the well thickness is comparable to the Zn

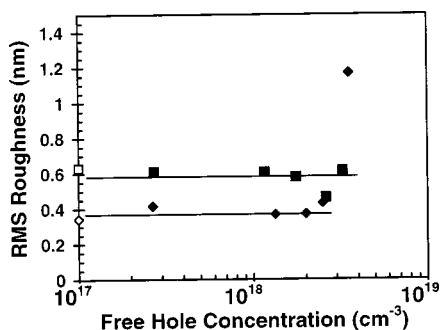


FIG. 6. rms roughness (from AFM measurements on a $1 \times 1 \mu\text{m}^2$ area) vs free hole concentration from Zn doping for both singular (001) (◆) and vicinal (■) layers. Data for undoped GaInP layers with *n*-type concentrations of $4.8 \times 10^{16} \text{ cm}^{-3}$ (singular, ◇) and $4.2 \times 10^{16} \text{ cm}^{-3}$ (vicinal, □) are included for comparison.

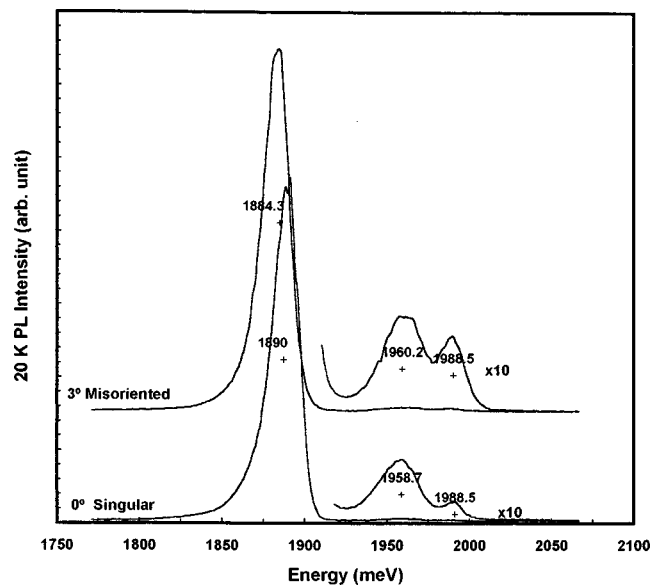


FIG. 7. PL spectra, measured at 20 K and an excitation intensity of 10 mW, for GaInP well structures grown at 670 °C for singular (001) (a) and vicinal (b) substrates. Each well structure is composed of a 300 nm disordered base layer, a 50 nm ordered well, and a 50 nm disordered cap layer. The disordered barrier layers are expected to have a Zn concentration of $\sim 2 \times 10^{18} \text{ cm}^{-3}$ which causes disordering.

diffusion length, $2\sqrt{Dt}$, during the growth process, where *D* is the Zn diffusion coefficient and *t* is the growth time measured from the beginning of growth of the well layer to the end of the growth run.

DISCUSSION

Recently published results for Te-doped GaInP layers grown in the same OMVPE apparatus showed that the step structure and ordering are markedly changed by the addition of Te, beginning at a level of approximately $3 \times 10^{17} \text{ cm}^{-3}$.¹⁰⁻¹² The [110] step spacing was observed to increase by over an order of magnitude with increasing doping level, while the step spacing between [110] steps increased only slightly.¹¹ A model was proposed for the coincident change in step structure and the degree of order based on the effect of Te on the step structure and adatom bonding at the step edges.¹⁰

The results for Zn-doped GaInP presented here are very different. The degree of order for vicinal layers versus doping level for Te and Zn are compared in Fig. 8. Disorder clearly occurs at a significantly smaller doping level for Te than for Zn. A second difference is that the Zn doping levels that produce disordering cause only minor effects on the step spacing (either [110] or [110] steps). The [110] step spacing is decreased slightly by Zn at concentrations exceeding 10^{18} cm^{-3} . This can be explained in terms of the elimination of “dangling” P atoms at [110] steps¹⁰ by Zn, which has one fewer valence electron. The average step height and rms roughness are virtually unchanged over the range of doping that produces disordering. It appears as though the disordering mechanism induced by Zn does not involve the steps. This may be because Te is a surfactant, as observed on GaAs surfaces during molecular-beam epitaxy growth,³⁰ i.e., it ac-

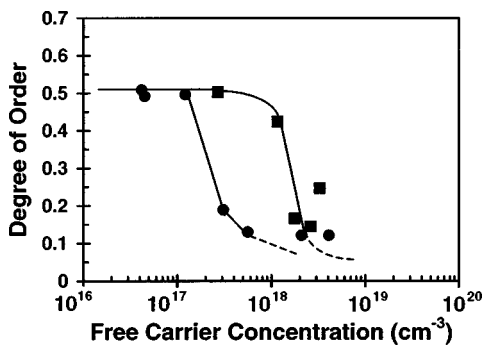


FIG. 8. Degree of order vs free carrier (electron for Te, hole for Zn) concentration from intentional Te (●) or Zn (■) doping. All data are for GaInP (001) vicinal layers grown at 670 °C. Results for undoped GaInP (001) vicinal layers (□) are shown for comparison. The lines were simply drawn through the data points.

cumulates at the surface. The Te concentration is apparently especially high at $[\bar{1}10]$ step edges. In contrast the Zn on the surface readily evaporates. In addition, it is expected to diffuse rapidly from the surface into the bulk.

There are several factors, other than adatom attachment kinetics at steps during growth, that might cause the disordering. A reduction in the thermodynamic driving force for ordering due to a reduction in the concentration of $[\bar{1}10]$ -oriented P dimers on the (2×4) -like reconstructed surface can cause a decrease of order parameter.³¹ For Te-doped GaInP, however, the reduction in ordering is apparently not caused by a change in the surface reconstruction.¹¹ In addition, the disordering of the sandwiched, undoped layers in the QW structures discussed in the last section was obviously caused by Zn diffusion in the *bulk*, not by destabilization of the *surface* reconstruction or any other process occurring at the surface during growth. This suggests that this is not the cause of disordering, although the actual surface reconstruction during growth could not be measured because Zn clouded the windows in the surface photo absorption apparatus.

A likely mechanism for the disordering induced by doping is that high acceptor concentrations increase the diffusion coefficients of Ga and In atoms in the bulk due to the change in Fermi level. For this mechanism, the movement of the Fermi level due to *p*-type doping would increase the concentrations of the charged point defects that contribute to interdiffusion of the group III atoms. This has been observed in AlAs/GaAs superlattices.^{32,33} Note that the doping level and doping type (*n* or *p*) are important, but the effect is independent of dopant species.

Another possible mechanism for an increase in the group III diffusion coefficients due specifically to Zn doping is the kick-out mechanism.^{34,35} There is some evidence to support the model of increased intermixing of group III atoms by Zn diffusion in III/V heterostructures. Secondary ion mass spectrometry and Auger electron spectroscopy studies show enhanced group III diffusion caused by Zn in AlGaAs/GaAs,^{36–38} GaInAsP/InP,^{39–41} GaInAsP/GaAs,⁴² AlGaInP/GaAs,⁴³ and InGaAs/InAlAs.⁴⁴ For AlAs/GaAs superlattices with a Zn-diffused doping level of 10^{18} cm^{-3} at 600 °C, the Ga–Al interdiffusion coefficient was measured to

be approximately $10^{-16} \text{ cm}^2/\text{s}$ ⁴⁵ which is about ten orders of magnitude higher than the extrapolated Ga–Al interdiffusion coefficient for the undoped materials at the same temperature.⁴⁶ In addition, a Ga–In interdiffusion coefficient of approximately $5 \times 10^{-14} \text{ cm}^2/\text{s}$ has been measured for GaInAsP layers with Zn-diffused doping levels of 10^{19} – $2 \times 10^{21} \text{ cm}^{-3}$ at 700 °C, which is many orders of magnitude higher than that expected for the undoped material at the same temperature.⁴²

An extrapolated interstitial Zn diffusion coefficient of $\sim 3 \times 10^{-16} \text{ cm}^2/\text{s}$ (from Zn diffusion in GaAs at 675 °C)⁴⁶ and a diffusion time typical of the growth of QWs in this work give a diffusion length of $\sim 9 \text{ nm}$. This is roughly consistent with the results: (i) a strong PL peak from the ordered layer is observed only the 50 nm wells, and not for the 5 and 10 nm QWs, and (ii) the well boundaries are fuzzy on a 10 nm scale for all the well structures examined in cross-sectional TEM.

SUMMARY

The step structure and CuPt ordering have been investigated in Zn-doped GaInP layers grown by OMVPE on singular and vicinal (3°_B misoriented) substrates at a growth temperature of 670 °C. The degree of order is estimated from the low temperature photoluminescence peak energy to be approximately 0.5 for undoped epitaxial layers and the layers are completely disordered at Zn doping concentrations of $> 1.7 \times 10^{18} \text{ cm}^{-3}$. This is verified by TED results. The band gap energy is increased by 110 meV as the Zn doping level is increased from 3×10^{17} to $1.7 \times 10^{18} \text{ cm}^{-3}$.

For single layers, the $[\bar{1}10]$ and $[110]$ -step spacings as well as the rms roughness are nearly unchanged over the range of Zn doping that produces disordering for both singular (001) and vicinal substrates. This suggests that the disordering caused by Zn doping does not involve a change in the step structure and adatom attachment dynamics as previously reported for Te. The disordering is believed to be caused by the interdiffusion of Ga and In due to the introduction of Zn.

Attempts were made to grow QW structures using the Zn to disorder the barrier layers. However, no apparent wells were observed for 5 and 10 nm wells by TEM and no QW-related optical transitions were detected in low temperature PL. This is believed to be due to the disordering of the well layer (expected to be ordered) due to Zn diffusion from the barrier layers into the well layer during growth. Both ordered and disordered regions were observed in wide, 50 nm wells.

ACKNOWLEDGMENTS

The authors would like to thank Prof. R. M. Cohen in University of Utah for his helpful discussions. This work was financially supported by the Department of Energy (OMVPE growth and TEM studies) and the National Science Foundation (AFM and PL studies).

¹G. B. Stringfellow, in *Common Themes and Mechanisms of Epitaxial Growth*, edited by P. Fuoss, J. Tsao, D. W. Kisker, A. Zangwill, and T. Kuech (Materials Research Society, Pittsburgh, 1993), pp. 35–46.

²S. B. Zhang, S. Froyen, and A. Zunger, *Appl. Phys. Lett.* **67**, 3141 (1995).

- ³L. C. Su, I. H. Ho, N. Kobayashi, G. B. Stringfellow, *J. Cryst. Growth* **145**, 140 (1994).
- ⁴A. Zunger and S. Mahajan, in *Handbook on Semiconductor*, edited by T. S. Moss (Elsevier Science B.V., Amsterdam, 1994), p. 1399.
- ⁵Y. S. Chun, S. H. Lee, I. H. Ho, and G. B. Stringfellow, *J. Cryst. Growth* **174**, 585 (1997).
- ⁶Y. S. Chun, S. H. Lee, I. H. Ho, and G. B. Stringfellow, *J. Appl. Phys.* **81**, 646 (1997).
- ⁷H. Murata, I. H. Ho, Y. Hosokawa, and G. B. Stringfellow, *Appl. Phys. Lett.* **68**, 2237 (1996).
- ⁸A. Gomyo, H. Hotta, I. Hino, S. Kawata, K. Kobayashi, and T. Suzuki, *Jpn. J. Appl. Phys., Part 2* **28**, L1330 (1989).
- ⁹J. P. Goral, S. R. Kurtz, J. M. Olson and A. Kibbler, *J. Electron. Mater.* **19**, 95 (1990).
- ¹⁰S. H. Lee, C. Y. Fetzer, G. B. Stringfellow, D. H. Lee, and T. Y. Seong, *J. Appl. Phys.* **85**, 3590 (1999).
- ¹¹S. H. Lee, T. C. Hsu, and G. B. Stringfellow, *J. Appl. Phys.* **84**, 2618 (1998).
- ¹²S. H. Lee, C. Y. Fetzer, and G. B. Stringfellow, *J. Cryst. Growth* **195**, 13 (1998).
- ¹³C. H. Wu, M. S. Feng, and C. C. Wu, *Mater. Res. Soc. Symp. Proc.* **300**, 477 (1993).
- ¹⁴A. Gomyo, T. Suzuki, K. Kobayashi, S. Kawata, I. Hino, and T. Yuasa, *Appl. Phys. Lett.* **50**, 673 (1987).
- ¹⁵S. R. Kurtz, J. M. Olson, D. J. Friedman, A. E. Kibbler, and S. Asher, *J. Electron. Mater.* **23**, 431 (1994).
- ¹⁶E. Morita, M. Ikeda, O. Kumagai, and K. Kaneko, *Appl. Phys. Lett.* **53**, 2164 (1988).
- ¹⁷F. P. Dabkowski, P. Gavrilovic, K. Meehan, W. Stutius, J. E. Williams, M. A. Shahid, and S. Mahajan, *Appl. Phys. Lett.* **52**, 2142 (1998).
- ¹⁸T. Suzuki, A. Gomyo, I. Hino, K. Kobayashi, S. Kawata, and S. Iijima, *Jpn. J. Appl. Phys., Part 2* **27**, L1549 (1988).
- ¹⁹M. K. Lee, R. H. Horng, and L. C. Haung, *Appl. Phys. Lett.* **59**, 3261 (1991).
- ²⁰M. Kondo, C. Anayama, N. Okada, H. Sekiguchi, K. Domen, and T. Tanahashi, *J. Appl. Phys.* **76**, 914 (1994).
- ²¹M. Ikeda and K. Kaneko, *J. Appl. Phys.* **66**, 5285 (1989).
- ²²C. C. Hsu, J. S. Yuan, R. M. Cohen, and G. B. Stringfellow, *J. Appl. Phys.* **59**, 395 (1986).
- ²³T. Iwamoto, K. Mori, M. Mizuta, and H. Kukimoto, *J. Cryst. Growth* **68**, 27 (1984).
- ²⁴G. B. Stringfellow, *Organometallic Vapor-Phase Epitaxy: Theory and Practice*, 2nd ed. (Academic, San Diego, 1999), pp. 91–95.
- ²⁵P. Ernst, C. Geng, F. Scholze, H. Schweizer, Y. Zhang, and A. Mascarenhas, *Appl. Phys. Lett.* **67**, 2347 (1994).
- ²⁶J. I. Pankove, *Optical Processes in Semiconductors* (Dover, New York, 1971), p. 134.
- ²⁷H. C. Casey, Jr. and F. Stern, *J. Appl. Phys.* **47**, 631 (1976).
- ²⁸L. C. Su, I. H. Ho, and G. B. Stringfellow, *J. Appl. Phys.* **75**, 5135 (1994).
- ²⁹S. H. Lee and G. B. Stringfellow, *J. Appl. Phys.* **83**, 3620 (1998).
- ³⁰N. Grandjean, J. Massies, and V. H. Etgens, *Phys. Rev. Lett.* **69**, 796 (1992); J. Massies, N. Grandjean, and V. H. Etgens, *Appl. Phys. Lett.* **61**, 99 (1992).
- ³¹H. Murata, I. H. Ho, L. C. Su, Y. Hosokawa, and G. B. Stringfellow, *J. Appl. Phys.* **79**, 6895 (1996).
- ³²T. Y. Tan and U. Gosele, *J. Appl. Phys.* **61**, 1841 (1987).
- ³³T. Y. Tan and U. Gosele, *Mater. Chem. Phys.* **44**, 45 (1996).
- ³⁴U. Gosele and Morehead, *J. Appl. Phys.* **52**, 4617 (1981).
- ³⁵R. M. Cohen, *Mater. Sci. Eng., R.* **20**, 167 (1997).
- ³⁶N. Hong Ky, J. D. Ganiere, M. Gailhanou, B. Blanchard, L. Pavesi, G. Burri, D. Araujo, and F. K. Reinhart, *J. Appl. Phys.* **73**, 3769 (1993).
- ³⁷J. W. Lee and W. D. Laidig, *J. Electron. Mater.* **13**, 147 (1984).
- ³⁸D. G. Deppe and N. Holonyak, Jr., *J. Appl. Phys.* **64**, R93 (1988).
- ³⁹K. Nakashima, Y. Kawaguchi, Y. Kawamura, Y. Imamura, and H. Asahi, *Appl. Phys. Lett.* **52**, 1383 (1988).
- ⁴⁰S. A. Schwarz *et al.*, *Appl. Phys. Lett.* **53**, 1051 (1988).
- ⁴¹G. J. van Gurp, W. M. van de Wijgert, G. M. Fontijn, and P. J. A. Thijs, *J. Appl. Phys.* **67**, 2919 (1990).
- ⁴²H. H. Park, K. H. Lee, and D. A. Steven, *Appl. Phys. Lett.* **53**, 2299 (1988).
- ⁴³D. G. Deppe *et al.*, *Appl. Phys. Lett.* **52**, 1413 (1988).
- ⁴⁴R. J. Baird, T. J. Potter, R. Lai, G. P. Kothiyal, and P. K. Bhattacharya, *Appl. Phys. Lett.* **53**, 2302 (1988).
- ⁴⁵T. Y. Tan and U. Gosele, *Appl. Phys. Lett.* **52**, 1240 (1988).
- ⁴⁶S. Reynolds, D. W. Vook, and J. F. Gibbons, *J. Appl. Phys.* **63**, 1052 (1988).